



The University of Bradford Institutional Repository

<http://bradscholars.brad.ac.uk>

This work is made available online in accordance with publisher policies. Please refer to the repository record for this item and our Policy Document available from the repository home page for further information.

To see the final version of this work please visit the publisher's website. Access to the published online version may require a subscription.

Link to publisher's version: <https://doi.org/10.1016/j.surfcoat.2017.11.003>

Citation: Seyedin SH, Ardjmand M, Safekordi AA et al (2018) Using response surface methodology to optimize the operating parameters in a top-spray fluidized bed coating system. *Surface and Coatings Technology*. 334: 43-49.

Copyright statement: © 2017 Elsevier. Reproduced in accordance with the publisher's self-archiving policy. This manuscript version is made available under the [CC-BY-NC-ND 4.0 license](https://creativecommons.org/licenses/by-nc-nd/4.0/).



Using Response Surface Methodology to Optimize the Operating Parameters in a Top-spray Fluidized Bed Coating System

Seyed Hadi Seyedin¹, Mehdi Ardjmand², Ali Akbar Safekordi¹, Shahram Raygan³, Ehsan Zhalehrajabi^{4*}, Nejat Rahmanian⁵

¹Department of chemical engineering, science and research branch, Islamic Azad University, Tehran, Iran.

²Department of chemical engineering, south Tehran branch, Islamic Azad University, Tehran, Iran.

³School of metallurgy and materials engineering, college of engineering, University of Tehran, Tehran, Iran.

⁴Department of chemical engineering, Universiti Teknologi PETRONAS, Bandar Seri Iskandar, Perak, Malaysia.

⁵Chemical engineering, faculty of engineering and informatics, University of Bradford, UK.

*Corresponding author: To whom correspondence should be addressed to E. Zhalehrajabi, email:e.zhaleh@gmail.com; ehsan_g02908@utp.edu.my, Phone: +601135616656.

Abstract

The fluidized bed coating system is a conventional process of particles coating in various industries. In this work, an experimental investigation was conducted using Response Surface Methodology (RSM) to optimize the coating mass of particles in a top-spray fluidized bed coating. The design of experiments (DOE) is a useful tool for controlling and optimization of products in industry. Thus, DOE was conducted using MINITAB software, version 16. This process used a sodium silicate solution for coating the sodium percarbonate particles. The effect of the fluidization air flow rate, atomization air flow rate and liquid flow rate on the coating mass in the top-spray fluidized bed coating was investigated. The experimental results indicated that the coating mass of particles is directly proportional to the liquid flow rate of the coating solution and inversely proportional to the air flow rate. It was demonstrated that the flow rate of the coating solution had the greatest influence on the coating efficiency.

Keywords

Fluidized bed, Top-spray Coating, Pneumatic nozzle, RSM.

1 Introduction

Fluidized bed technology is a common process step in the chemical, agricultural, pharmaceutical and food industries. The coating of solid particles, among others, is used to achieve a variety of functions, including the controlled release of drugs, protection of the core from external conditions, taste or odor masking, easier powder handling, and greater stability [1-3]. In addition, the fluid bed

coating technique has been used in drug delivery systems [4]. Fluidized beds are divided into top-spray, tangential spray, bottom spray and the Wurster system (this is used more in the pharmaceutical industry). The coating of high-quality particles is often done using the top-spray system with a circulating fluid (see Fig. 1). In this system, a cylinder of appropriate size is placed in the center of the bed. The system forces the particles to circulate in the bed, which facilitates an even distribution of the wetting and drying time between particles [5,6]. In the top-spray fluidized bed coating, the coating solution is sprayed onto the surface of the fluidizing particles by a nozzle which is placed above the bed. The coating solution that is adhesive on the particle surface is dried due to the heat and vapor removal supplied by the fluidizing gas. The advantage of this coating technique is that the coating and drying take place simultaneously. Moreover, it can be used to coat particles in the size range of 0.1 to several millimeters [7]. The product quality and the process efficiency are largely determined by the spray and bed characteristics, and the particle motion characteristics in terms of the residence and circulation times [8, 9]. For spraying liquid droplets in a fluid bed, generally, pneumatic two-fluid nozzles are used. In these nozzles, the liquid jet is changed to droplets by the air flow. Using pneumatic nozzles helps to control the size and distribution of the droplets, particularly when the liquid flow rate is low. the droplets sprayed by the pneumatic two-fluid nozzles are smaller than those using single fluid nozzles. The important aspects in controlling the fluidized bed coating process include controlling the product temperature and the growth of the coating film. Applying a fluidized bed coating to heat sensitive products,

such as enzymes, proteins or microorganisms, can protect them from environmental damage [1, 10-12].

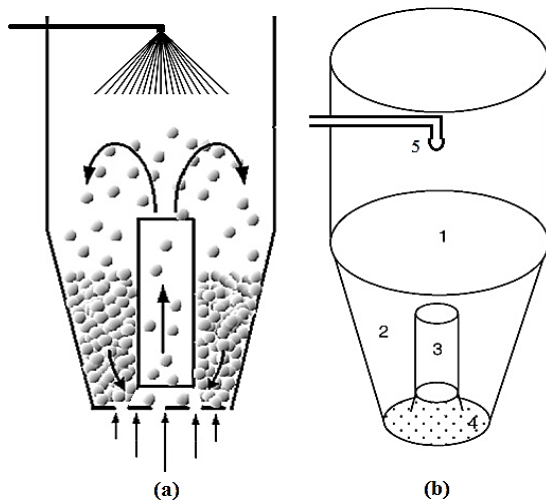


Fig. 1 a) Schematic image of a top-spray system with circulating fluid. b) Different parts of the bed: 1. Expansion chamber (deceleration region, fountain), 2. Down bed region, 3. Draft tube (Cylinder), 4. Air distributor plate, 5. Nozzle.

The tools and techniques used in the DOE have proven successful in meeting the challenge of continuous improvement in many manufacturing organizations over the last two decades. However, research has shown that the application of this powerful technique in many companies is limited due to the lack of statistical knowledge required for its effective implementation [13]. Within the DOE approach, initially a target value or set of target values has to be defined for specific parameters, which is referred to as the response. To become acquainted with a process, in general, DOE uses a screening design to analyze the effect of several influencing variables on the response and to separate the main influencing parameters from those that only have a minor impact. A further step within the DOE approach is the response surface methodology, which investigates the local and global optima of the process and identifies the relevant interactions between the influencing variables [14]. DOE is one of the key elements of the quality by design principles that have been used to study fluidized bed coating process. The use of DOE allows for testing a large number of factors, as well as their interactions simultaneously. The response surface methodology (RSM) is one of the popular methods in DOE, which involves the use of different types of experimental design to generate polynomial mathematical relationships and to map the response over the experimental domain to select the optimal process parameters [15, 16, 17]. An efficient way of planning and optimizing such experiments involves

the principles of DOE. The key property of DOE is that while several factors are varied simultaneously, each factor may be evaluated independently. The simplest DOE are often factorial experiments, where all factors are varied simultaneously at a limited number of factor levels. More complex DOE involve response surface designs. Central Composite Designs (CCD) are possibly the most popular type of response surface designs [18]. If the factors act additively, the DOE design does the job with much more precision than one-factor-at-a-time methods, and if the factors do not act additively, the DOE, unlike the one-factor-at-a-time design, can detect and estimate the interactions that measure this non-additivity. Hence, an advantage of DOE is that it allows for the maximum amount of information to be extracted using the minimum number of experiments. DOE is also useful as it allows for straightforward handling of experimental errors and allows for data extrapolation [19]. The top-spray fluid bed system is used for particles coating. In this process, coating materials are sprayed onto the fluidized particles, and the liquid reacts with fluid particles or covers their surface in the bed [20]. The uniform distribution of the coat in the fluid bed depends on the type of coating liquid, size and type of particles being coated, fluidization air flow, and nozzle spray type [21, 22]. In the fluidized bed coating, agglomeration is an undesirable phenomenon, and a number of studies have focused on reducing it [23, 24]. Agglomeration is mostly used for pelletizing and granulation in the pharmaceutical industry [25]. In recent years, some work in the field of mathematical modeling and the simulation of hydrodynamics, heat and mass transfer in fluidized beds, and the droplet deposition behavior and dynamic particle populations in the granulation process have been conducted [8, 26-29]. Some studies have also addressed the optimization of various process parameters for the formulation and scaling parameters in fluid beds [30, 31]. Recently, statistical optimization was employed in the various processes because it quickly screens a number of multiple parameters and their interactions, and reflects the function of an individual factor or component [32]. In the present study, sodium percarbonate particles are coated by sodium silicate in a top-spray fluidized bed system. The protective silicate layer protects laundry detergent powder particles from humidity and corrosion and conserves the available oxygen in the powder, where oxygen has a bleaching role in the powder. The aim of this study is to recommend an

established statistical methodology to optimize the process conditions, such as the fluidization air flow rate, liquid flow rate, and the atomization air flow rate to enhance the coating mass using the RSM experimental design.

1.1 Materials and Method

Sodium percarbonate powder (SPC) was supplied from the Solvay company (OXYPER®, general grade, and available oxygen is minimum 30%). SPC particles were fractionated by sieving. The mean diameter of the particles (grade dependent) was in the range of 450 to 500 μm . For each coating experiment, 100 g of SPC was used. Sodium silicate (SS) solution was used as the coating solution with 30% volumetric concentration and diluted in water (300 ml liquid sodium silicate was dissolved in 700 ml water). The chemical composition of the applied materials is summarized in Table 1.

Table 1 General properties of materials.

| Name-Formula | Appearance | Density (kg/m ³) | MW(kg/mol) |
|---|-----------------------------------|------------------------------|------------|
| Sodium percarbonate $\text{Na}_2\text{CO}_3 \cdot 1.5\text{H}_2\text{O}_2$ | White solid | Water free 900 | 0.157 |
| Sodium silicate Na_2SiO_3 | White to greenish opaque crystals | 2610 | 0.122 |

2 Equipment

A Plexiglas fluidized bed chamber was used for the coating process. For spraying of the coating solution, a pneumatic nozzle was placed in the top of the bed. After the spraying process, the coated particles were dried in the bed. The process variables were the atomization air flow rate due to controlling the spray droplet size, the fluidization air flow rate, and the liquid flow rate of the coating solution.

2.1 Description of the Coating Process

The top-spray fluid bed coating system used in the present study is shown in Fig. 2. As shown in Fig. 2, the shape of the bed is cylindrical, the bed height is 450 mm, and the bed diameter is 170 mm. There is a small cylinder (draft tube with 70 mm width and 100 mm height) in the center of the bed, which provides a circular flow of particles for a better coating process. Also, there are three sensors

for controlling the temperature (S1, S2, S3) and one for humidity (S4). The air and liquid flow rates are measured by means of the rotameters.

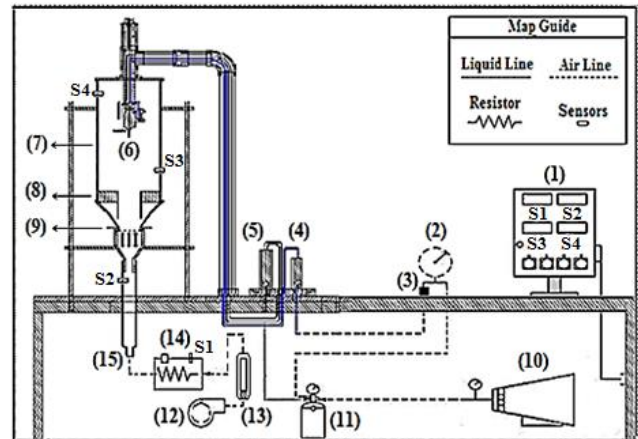


Fig. 2 Schematic image of the apparatus: 1. Power and control box, 2. Pressure gauge, 3. Electric valve, 4. Liquid Rotameter, 5. Atomization air Rotameter, 6. Nozzle, 7. Fluid bed, 8. Internal Cylinder, 9. Air distributor, 10. Air compressor, 11. Liquid pressure tank, 12. Blower, 13. Fluidization air Flowmeter, 14. Heater, 15. Inlet air Flow.

2.2 Process Performance

The air flow leaves the blower and enters into the bed via the air distributor plate located in the bottom of the bed. The compressed air goes into the nozzle to spray the coating liquid onto the fluidized particles. During each cycle, the coating liquid is sprayed on the fluidized particles before they are dried. This system is composed of three main parts:

1. A nozzle to spray the liquid.
2. An air distribution plate to fluidize the particles.
3. A draft tube to create the circulating flow.

During the fluidization process in the bed, the nozzle sprays the coating solution on the fluidized particles. In each experiment, the coating mass W_C (g) on the particles surface was measured and reported based on 100g sodium percarbonate particles. The liquid solution was sprayed three times per minute (each spray pulse was about 1 second). This regulates the coating value to prevent the adhesion or agglomeration of the particles in the bed. During the coating process, the temperature and humidity of the bed were measured and controlled. These variables help to improve the product quality. Decreasing the temperature causes an increase in the humidity and agglomeration may occur in the bed.

3 Experimental Design

To optimize the coating process in the fluidized bed, the response surface as a function of the selected key variables was determined. The coded and physical values of the investigated process variables were the atomization of the air flow rate (QA), liquid flow rate (QL) for spraying and the fluidization air flow rate (QF), which are illustrated in Table 2. The low level of the variables is (-1), medium level is (0), and high level is (+1).

Table 2 Actual and coded values of the process variables.

| Actual values | Low | Medium | High |
|-------------------------|-----|--------|------|
| QA (L/min) | 5 | 7.5 | 10 |
| QL (ml/min) | 25 | 62.5 | 100 |
| QF (m ³ /hr) | 150 | 375 | 600 |
| Coded values | -1 | 0 | +1 |

3.1 Analysis of the process

For each experiment, 100g anhydrous sodium percarbonate was coated on the floor of the bed, and then these particles were fluidized by the buoyancy force of the air and covered in 5 min by the spraying of liquid sodium silicate. After the coating process, the particles were dried by the hot air flow for 3 min. The particles mass was weighed before and after the coating stage. The normal temperature for drying the fluidized particles in the bed was set to 70 ° C as this is more than the dew point, and, hence, there will be no humidity in the product. During the drying process, the best temperature was controlled by a heater using a temperature controller. The bed humidity was evaluated before starting the coating process and after the drying process for better production. In some cases, due to high humidity in the bed, a viscous coating solution or the use of a high spray liquid flow rate during the coating process, some particles are converted to granular form (agglomerate) due to the coagulation and cohesion of the fluidized particles in the bed.

4 Results and Discussion

4.1 Coating Calculations

Before the experimental design, the maximum coating mass for a particle was calculated mathematically. The approximate mass of a particle, which is weighed using an accurate digital electronic precision balance (m_p) and the mass of 100g sodium percarbonate (m_t), which is divided by (m_p) to obtain the approximate number of particles (N) equals 34365. The mass of the coated particles

covered by sodium silicate solution is (m_s). Thus, the difference between the (m_s) and the coating mass for one particle is (m_c). The coating mass of one particle multiplied by N is used to calculate the maximum coating mass of 100g sodium percarbonate (W_{max}), which is equivalent to the mass of silicate in the suspension minus the mass of all the particles available to be coated. The value of the coating mass for 100g percarbonate particles after drying for each experiment is (W_C). The various stages of the calculation are as follows:

$$N = m_t/m_p = \frac{100\text{ g}}{2.91 \times 10^{-3}\text{ g}} = 34365 \quad (1)$$

$$m_c = m_s - m_p = 6.32 \times 10^{-4}\text{ g} \quad (2)$$

$$W_{max} = m_c \times N = 21.72\text{ g} \quad (3)$$

The experimental design, which includes three factors and levels for 20 runs, is reported in Table 3. MINITAB (Version 16.0) was used to describe the response surface method (RSM). RSM analysis was used to identify the optimum values of the experimental factors in a more effective way, and to reveal the important factor interactions.

Table 3 Experimental design and response values.

| N | QA | QL | QF | W _C (g) |
|----|----|----|----|--------------------|
| 1 | -1 | -1 | -1 | 13.00 |
| 2 | 1 | -1 | -1 | 11.74 |
| 3 | -1 | 1 | -1 | 18.45 |
| 4 | 1 | 1 | -1 | 16.80 |
| 5 | -1 | -1 | 1 | 12.10 |
| 6 | 1 | -1 | 1 | 11.40 |
| 7 | -1 | 1 | 1 | 17.80 |
| 8 | 1 | 1 | 1 | 15.00 |
| 9 | -1 | 0 | 0 | 14.20 |
| 10 | 1 | 0 | 0 | 13.50 |
| 11 | 0 | -1 | 0 | 11.74 |
| 12 | 0 | 1 | 0 | 17.54 |
| 13 | 0 | 0 | -1 | 14.15 |
| 14 | 0 | 0 | 1 | 13.56 |
| 15 | 0 | 0 | 0 | 13.90 |
| 16 | 0 | 0 | 0 | 13.80 |
| 17 | 0 | 0 | 0 | 14.00 |
| 18 | 0 | 0 | 0 | 14.10 |
| 19 | 0 | 0 | 0 | 14.00 |
| 20 | 0 | 0 | 0 | 13.85 |

The coating mass in various experiments and levels of liquid or air flow rates was analyzed using MINITAB software.

4.2 Results of RSM Analysis

An optimum coating mass is obtained of 18.614g for 100g of particles using RSM analysis. This

optimum value (W_{OP}) is close to the coating mass in experiment No.3 (18.45g) in Table 3. In this experiment, QA is 5 (L/min), QL is 100 (ml/min) and QF is 150 (m³/hr), which shows that the optimum coating mass is obtained for the maximum level of QL and the minimum level of QA and QF. Also, the responses of experiments 7 and 12 are close to the optimized value. Thus, increasing the liquid flow rate and decreasing the atomization and fluidization air flow rate, can achieve the optimal point. The relative error ratio, which is the difference between the optimum value (W_{op}) and achieved value in each experiment (W_i), can be calculated using equation 4.

$$\% \text{ Error} = \frac{|W_{OP} - W_i|}{W_{OP}} \times 100 \quad (4)$$

4.3 Analysis of Variance for Experiments

Analysis of variance (ANOVA) is used for better analysis of DOE and is complementary to the results. Table 4 shows the results of ANOVA for the coating mass (W_C). In the ANOVA table, DF is the degree of freedom, Seq SS (R^2) is sequential sum of squares, Adj SS is adjusted R-square, the F-value is a value, when we run an ANOVA test or a regression analysis to find out if the means between two populations are significantly different. Also F test will tell us, if a group of variables are jointly significant. We can use the F-value when deciding to support or reject the null hypothesis. We should also consider the P-value. The P-value is determined by the F-value. The F-value must be used in combination with the P-value. If we have a significant F-value, it doesn't mean that all your variables are significant. The statistic is just comparing the joint effect of all the variables together.

If the P-value is less than the alpha level, it should

be studied the individual P-values to find out which of the individual variables are statistically significant.

Otherwise our results are not significant and we cannot reject the null hypothesis. A common alpha level for tests is 0.05. The P-value is the measure of how likely the sample results are, assuming the null hypothesis is true. P-values range from 0 to 1. A small ($P < 0.05$, a commonly used level of significance) P-value indicates that the power level has a statistically significant effect on each rate. According to the results in column P, all three variables, fluidization air flow rate (QF), liquid flow rate (QL), and atomization air flow rate (QA) have a significant role in the response. However, the value of QL has the greatest impact on the result of the coating process, because the P-value for the interactions between the variables and QL is more significant. Thus, the liquid flow rate makes a direct contribution to the coating mass of the particle surface and the air flow rate is inversely proportional to the coating mass. Thus the increase of air flow rate, causes reduction of coating mass on the particles, because the F-value for liquid flow rate in ANOVA table is 589.56, that is the maximum value in column F. Also the R^2 value is 65.58 for the liquid flow rate, which shows that the liquid flow rate has more influence compared to the fluidization air flow rate and the atomization air flow rate.

The F-value and R^2 show the importance of the experimental model and confirm the experimental results. The minimum mean square error (MMSE) is 0.98548, which shows the accuracy of the results. Furthermore, the ANOVA results in the relevant columns for the R^2 and F-value have good consistency with the experimental data.

Table 4 Results of the ANOVA Table for coating mass, W_C (g).

| Source | DF | Seq SS | Adj SS | Adj MS | F | P |
|-------------|----|---------|---------|---------|--------|-------|
| Regression | 9 | 75.4904 | 75.4904 | 8.3878 | 75.40 | 0.000 |
| Linear | 3 | 72.3980 | 72.3980 | 24.1327 | 216.93 | 0.000 |
| QA | 1 | 5.0552 | 5.0552 | 5.0552 | 45.44 | 0.000 |
| QL | 1 | 65.5872 | 65.5872 | 65.5872 | 589.56 | 0.000 |
| QF | 1 | 1.7556 | 1.7556 | 1.7556 | 15.78 | 0.003 |
| Square | 3 | 2.0908 | 2.0908 | 0.6969 | 6.26 | 0.012 |
| QA*QA | 1 | 0.5314 | 0.0180 | 0.0180 | 0.16 | 0.696 |
| QL*QL | 1 | 1.5568 | 1.3827 | 1.3827 | 12.43 | 0.005 |
| QF*QF | 1 | 0.0026 | 0.0026 | 0.0026 | 0.02 | 0.881 |
| Interaction | 3 | 1.0015 | 1.0015 | 0.3338 | 3.00 | 0.082 |
| QA*QL | 1 | 0.7750 | 0.7750 | 0.7750 | 6.97 | 0.025 |

| | | | | | | |
|----------------|----|---------|--------|--------|------|-------|
| QA*QF | 1 | 0.0435 | 0.0435 | 0.0435 | 0.39 | 0.546 |
| QL*QF | 1 | 0.1830 | 0.1830 | 0.1830 | 1.65 | 0.229 |
| Residual Error | 10 | 1.1125 | 1.1125 | 0.1112 | | |
| Total | 19 | 76.6029 | | | | |

4.4 DOE Analysis Results

According to the Table 4, P-values were also considered as criteria for understanding the significance of the model. The smaller the value of P, the more significant the model is. P-values of more than 0.05 were identified as non-significant and non-contributing. The most significant effects of variables and their interactions were selected by considering the half-normal probability plots. Fig. 3 shows how these variables were selected. Red points (Circles) indicate main effects, whereas green points (Squares) indicate interactions. Values positioned away from the straight line and at the right side of the plot are significant modes which were used in the ANOVA calculations.

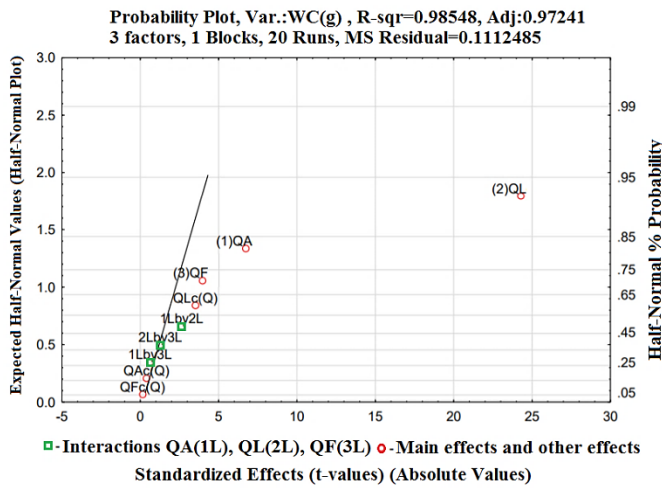


Fig. 3 Half-normal graphs for selecting the main effects QA(1L), QL(2L), QF(3L), interactions (1L by 2L, 2L by 3L, 1L by 3L) and Quadratic form QAc(Q), QLc(Q), QFc(Q).

The results and influence of the operational variables, atomization air flow (QA), liquid flow rate (QL) and fluidization air flow rate (QF), and the optimum values (OP) as contour lines by RSM analysis are shown in Figs. 4, 5 and 6.

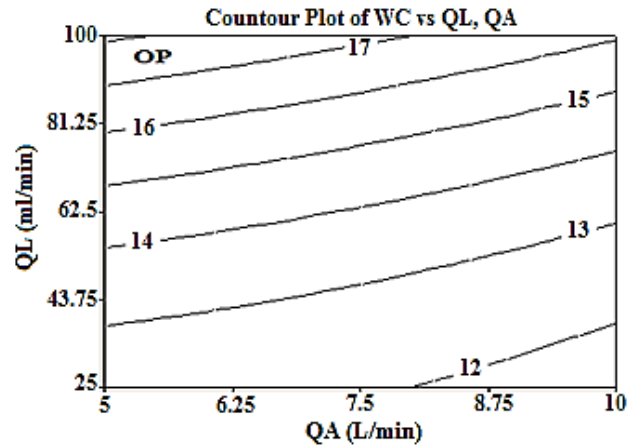


Fig. 4 Contour plot of the coating mass, W_C (g) as function of QA (L/min) and QL (ml/min).

As shown in Fig. 4, the reduction in the atomization air flow rate and the increase in the liquid flow rate cause an increase in the coating mass. Fig. 5 shows that a decrease in the fluidization air and atomization air flow rates increase the coating mass value. This is because of the reduction in the movement of the fluidized particles in the bed and the increase in the number of particles to be coated. An increase in the fluidization flow rate will result in faster particles movement, and, hence, less liquid sticks to them.

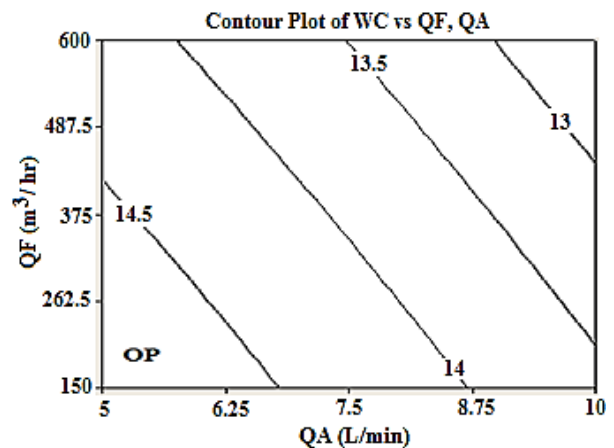


Fig. 5 Contour plot of the coating mass, W_C (g) as function of QA (L/min) and QF (m³/h).

An increase in the atomized air flow rate causes a decrease in the amount of liquid flowing through the nozzle orifice, and considerably less solution is poured on the particles. Thus, the effect of the liquid flow rate on the coating mass is positive, and the effect of air flow rate is negative. However, a

high liquid flow rate has a negative effect on the coating process and causes high humidity in the bed and particles agglomeration, and the product will be damaged.

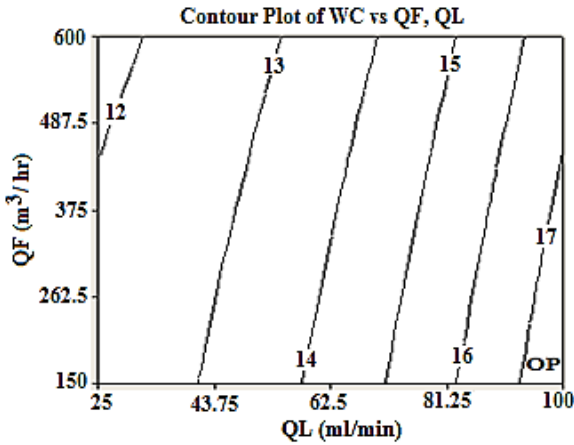


Fig. 6 Contour plot of the coating mass, W_C (g) as function of Q_F (m^3/h) and Q_L (ml/min).

As shown in Fig. 6, increasing the liquid flow rate and decreasing the fluidization air flow rate, increases the coating mass value, since the liquid spray rate decreases in the nozzle outlet and less coating solution is poured on the particles. An increase in the fluidization air flow rate, causes the particles to float more and move faster, and, hence, less liquid sticks to them, i.e., the optimized area is located on the far right at the bottom of Fig. 6.

The achieved results of the coating plots confirm that the liquid flow rate is the most effective relevant factor when aiming to increase the coating mass.

4.5 Regression Analysis

The regression coefficient, standard error, T-values and P-values for the full quadratic model of the coating mass are presented in Table 5. The fitted second-order polynomial is more acceptable. The total coating mass for 100g of particles is calculated using the second-order polynomial equation predicted by the model for maximum coating mass and by applying the regression analysis on the experimental data according to Table 5. The significance test of the individual model coefficients involves the determination of the P and T-values. The T-value represents the significance of the independent variables on the response. The P-value indicates that the three main factors and two interactions have a statistically significant effect on the

response. This shows that the factors $QA*QA$, $QF*QF$, $QA*QF$ and $QL*QF$ are not effective on the coating mass.

Table 5 Results of estimated regression for coating mass.

| Term | Coef | SE Coef | T | P |
|----------|---------|---------|---------|-------|
| Constant | 13.9374 | 0.1147 | 121.551 | 0.000 |
| QA | -0.7110 | 0.1055 | -6.741 | 0.000 |
| QL | 2.5610 | 0.1055 | 24.281 | 0.000 |
| QF | -0.4190 | 0.1055 | -3.973 | 0.003 |
| QA*QA | -0.0809 | 0.2011 | -0.402 | 0.696 |
| QL*QL | 0.7091 | 0.2011 | 3.526 | 0.005 |
| QF*QF | -0.0309 | 0.2011 | -0.154 | 0.881 |
| QA*QL | -0.3112 | 0.1179 | -2.639 | 0.025 |
| QA*QF | -0.0738 | 0.1179 | -0.625 | 0.546 |
| QL*QF | -0.1512 | 0.1179 | -1.283 | 0.229 |

A quadratic model was derived, of which all effects (first, second-order, and interaction) remained significant after model reduction ($P < 0.05$). Consequently, the following equation was obtained:

$$W_c = +13.9374 - 0.7110 QA + 2.5610 QL - 0.419 QF + 0.7091 QL^2 - 0.3112 QA \cdot QL - 0.1512 QL \cdot QF - 0.0738 QA \cdot QF - 0.0809 QA^2 - 0.0309 QF^2 \quad (5)$$

The coefficient of QL is 2.25 in Eq. (5); thus, the liquid flow rate has a greater impact on the amount of coating than the other coefficients. To obtain the optimum levels of the factors, given values were set by the MINITAB multiple response optimizer under global solution for the optimum levels of QA, QL and QF, which were 5 (-1), 100 (1) and 150 (-1), respectively; as shown in Table 6.

Table 6 Derived optimum levels for experimental variables.

| No. | QA (L/min) | QL (ml/min) | QF (m^3/hr) | Response (g) | Desirability (g) |
|-----|------------|-------------|-----------------|--------------|------------------|
| 3 | 5 | 100 | 150 | 18.45 | 18-19 |

The average total mass of coating from the results of column (W_C) in table 3 is 14.236g. The maximum response for the coating particles calculated using the RSM method is 18.45g. Thus, the coating yield is calculated using Eq. (6).

$$Yield = \left| \frac{14.236}{18.45} \right| \times 100 = 77.16 \% \quad (6)$$

Fig. 7 shows the Pareto chart of the standardized effects. The Pareto chart displays the absolute value of the effects and draws a reference line on the chart. Any effect that extends beyond this reference line is potentially important. According to the Pareto chart, factors QL, QA, QF, QL*QL and QA*QL have a significant effect on the response. Since the other terms are insignificant, we can drop these terms in the model.

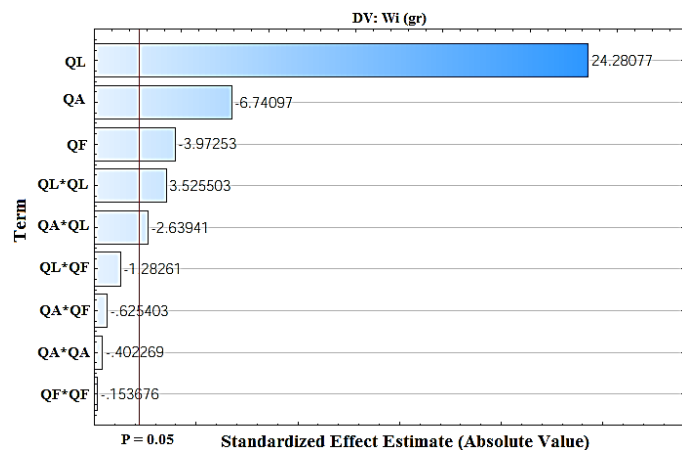


Fig. 7 Pareto chart of standardized effects.

Table 7 shows the fitted values, residuals and standardized residuals of the coating mass results.

Table 7 The normalized results of responses.

| StdOrder | W _c | Fit | Residual | Std Resid |
|----------|----------------|--------|----------|-----------|
| 1 | 13.00 | 12.567 | 0.433 | 2.85 |
| 2 | 11.74 | 11.915 | -0.175 | -1.16 |
| 3 | 18.45 | 18.614 | -0.164 | -1.08 |
| 4 | 16.80 | 16.717 | 0.083 | 0.54 |
| 5 | 12.10 | 12.179 | -0.079 | -0.52 |
| 6 | 11.40 | 11.232 | 0.168 | 1.11 |
| 7 | 17.80 | 17.621 | 0.179 | 1.18 |
| 8 | 15.00 | 15.429 | -0.429 | -2.83 |
| 9 | 14.20 | 14.567 | -0.367 | -1.54 |
| 10 | 13.50 | 13.145 | 0.355 | 1.49 |
| 11 | 11.74 | 12.085 | -0.345 | -1.45 |
| 12 | 17.54 | 17.207 | 0.333 | 1.40 |
| 13 | 14.15 | 14.325 | -0.175 | -0.74 |
| 14 | 13.65 | 13.487 | 0.163 | 0.68 |
| 15 | 13.90 | 13.937 | -0.037 | -0.12 |
| 16 | 13.80 | 13.937 | -0.137 | -0.44 |
| 17 | 14.00 | 13.937 | 0.063 | 0.20 |
| 18 | 14.10 | 13.937 | 0.063 | 0.52 |
| 19 | 14.10 | 13.937 | 0.063 | 0.20 |
| 20 | 13.85 | 13.937 | -0.087 | -0.28 |

4.6 Validation of the RSM Model

The significance test for the regression model was done using the ANOVA table and the results for the coating mass. The predicted model was validated to test the fitness of the model for further utilization. The predicted values matched with the experimental data reasonably well (Table 3), which indicated the good prediction accuracy and generalization ability of the predicted model. The higher coefficient values of multiple regression, R^2

(98.548%) and adjusted R^2 (97.241%) indicated the fitness and adequacy of the model. Moreover, the reduced model is obtained from table 5 and according to P factor is as follows:

$$W_c = 13.9374 - 0.711QA + 2.561QL - 0.419QF + 0.7091QL^2 - 0.3112QAQL \quad (7)$$

5 Conclusions

This paper has presented a systematic and up to date review of the fluidized bed coating method and presentation of the applications of the top-spray fluidized bed coating system. The effect of the important variables in the coating process was investigated. The RSM results showed that the mass of the coating layer around the particles was directly proportional to the liquid flow rate and inversely related to the atomization and fluidization air flow rates. The optimization of the physical conditions for the operational variables enhanced the coating mass in the fluidized bed coating process. The optimized responses confirmed that the optimum results for 18.614g coating mass were obtained with 100(ml/min) liquid flow rate, 150(m³/h) fluidization air flow rate and 5(L/min) atomization air flow rate. The RSM design revealed significant second order effects of the coating mass. The validity of the model was verified by fitting the values of the independent variables into the regression model equation. The nozzle liquid flow rate was demonstrated as having greater influence than the other variables on the coating mass. Thus, it appears that the flow rate of the coating solution plays an important role in determining the coating efficiency. In conclusion, coating losses can be reduced drastically by the selection of appropriate processing conditions. Future research can focus on temperature variations and the pressure drop along the bed.

Acknowledgments

This work was funded by the Metallic Material Processing Research Group, ACECR, Branch of Tehran University, Tehran, Iran. The researchers wish to express their gratitude for the technical support given by Seyed Hasan Alhoseini.

References

- [1] Krupa, A., Jachowicz, R., Kurek, M., Figiel, W., Kwiecień, M. "Preparation of solid self-emulsifying drug delivery systems using magnesium aluminometasilicates and fluid-bed coating process." *Powder Technol.* 266, pp. 329-339. 2014.
DOI: [10.1016/j.powtec.2014.06.043](https://doi.org/10.1016/j.powtec.2014.06.043)
- [2] Šibanc, R., Srčič, S., Dreu, R. "Numerical simulation of two-phase flow in a Wurster coating chamber and comparison with experimental results." *Chem. Eng. Sci.* 99, pp. 225-237. 2013.
DOI: [10.1016/j.ces.2013.05.057](https://doi.org/10.1016/j.ces.2013.05.057)
- [3] Karlsson, S., Rasmuson, A., Niklasson Björn, I., Schantz, S. "characterization and mathematical modelling of single fluidised particle coating." *POWDER TECHNOLOGY.* 207, pp. 245-256. 2011.
DOI: [10.1016/j.powtec.2010.11.006](https://doi.org/10.1016/j.powtec.2010.11.006)
- [4] Rieck, C., Hoffmann, T., Bück, A., Peglow, M., Tsotsas, E., "Influence of drying conditions on layer porosity in fluidized bed spray granulation." *Powder Technol.* 272, pp. 120-131. 2015.
DOI: [10.1016/j.powtec.2014.11.019](https://doi.org/10.1016/j.powtec.2014.11.019)
- [5] Kage, H., Dohzaki, M., Hironao Ogura, Yoshizo Matsuno. "powder coating efficiency of small particles and their agglomeration in circulating fluidized bed." *Korean J. Chem. Eng.* 16, pp. 630-634. 1999.
DOI: [10.1007/BF02708143](https://doi.org/10.1007/BF02708143)
- [6] Hede, P.D., Jensen, A.D., Bach, P. "Small-scale top-spray fluidised bed coating: Granule impact." *Powder Technol.* pp. 156–167. 2007.
DOI: [10.1016/j.powtec.2007.02.018](https://doi.org/10.1016/j.powtec.2007.02.018)
- [7] Palamanit, A., Soponronnarit, S., Prachayawarakorn, S., Tungtrakul, P. "Effects of inlet air temperature and spray rate of coating solution on quality attributes of turmeric extract coated rice using top-spray fluidized bed coating technique." *J. Food Eng.* 114, pp. 132-138. 2013.
DOI: [10.1016/j.jfoodeng.2012.07.014](https://doi.org/10.1016/j.jfoodeng.2012.07.014)
- [8] Depypere, F., Pieters, G., Dewettinck, K. "CFD analysis of air distribution in fluidised bed equipment." *Powder Technology.* 145, pp. 176–189. 2004.
DOI: [10.1016/j.powtec.2004.06.005](https://doi.org/10.1016/j.powtec.2004.06.005)
- [9] Vanderroost, M., Ronsse, F., Dewettinck, K., Pieters, J. "Modelling overall particle motion in fluidised beds for top-spray coating processes." *Particuology journal.* 11, pp. 490-505. 2013.
DOI: [10.1016/j.partic.2012.07.012](https://doi.org/10.1016/j.partic.2012.07.012)
- [10] Ronsse, F., Pieters, J.G., Dewettinck, K. "Modelling side-effect spray drying in top-spray fluidised bed coating processes." *J. Food Eng.* 86, pp. 529-541. 2008.
DOI: [10.1016/j.jfoodeng.2007.11.003](https://doi.org/10.1016/j.jfoodeng.2007.11.003)
- [11] Silva, O. S., Rocha, S. C. S., Marsal, S. C. "The influence of the moisture content of microcrystalline cellulose on the coating process in a fluidized bed." *Braz. J. Chem. Eng.* 21, 2, 2004.
DOI: [10.1590/S0104-66322004000200023](https://doi.org/10.1590/S0104-66322004000200023)
- [12] Shelukar, S., Ho, J., Zega, J., Roland, E., Yeh, N., Quiram, D., Nole, A., Katdare, A., Reynolds, S. "Identification and characterization of factors controlling tablet coating uniformity in a Wurster coating process." *Powder Technol.* 110, pp. 29-36. 2000.
DOI: [10.1016/S0032-5910\(99\)00265-X](https://doi.org/10.1016/S0032-5910(99)00265-X)
- [13] Antoy, J., *Design of Experiments for Engineers and Scientists*, (2nd ed), John Willy publication, 2014.
- [14] Diamond, W. J., *Practical Experiment Designs*, John Wiley and Sons, 2001.
- [15] Liu, H., Wang, K., Schlindwein, W., Li, M., "Using the Box–Behnken experimental design to optimise operating parameters in pulsed spray fluidised bed granulation." *Int. J. Pharm.* 448, pp. 329-338. 2013.
DOI: [10.1016/j.ijpharm.2013.03.057](https://doi.org/10.1016/j.ijpharm.2013.03.057)
- [16] Dewettinck, K., Huyghebaert, A. "Top-Spray Fluidized Bed Coating: Effect of Process Variables on Coating Efficiency." *Food Sci. Technol. Int.* 31, pp. 568-575. 1998.
DOI: [10.1006/fstl.1998.0417](https://doi.org/10.1006/fstl.1998.0417)
- [17] Eldeen, K. I., Ibrahim, H.M., Elkhidir, E. E., Elamin, H. B., "Optimization of culture conditions to enhance nattokinase production using RSM." *American Journal of Microbiological Research.* 3(5), pp. 165-170. 2015.
DOI: [10.12691/ajmr-3-5-3](https://doi.org/10.12691/ajmr-3-5-3)
- [18] Box, G. E. P., Hunter, J. S., Hunter, W. G., Hoboken, N. J., *Statistics for experimenters: design, innovation, and discovery* (2nd ed.), John Willy publication, 2005.
- [19] Vanaja, K., Rani, R.H. S., *Design of experiments: Concept and Applications of Plackett Burman design Clinical Research and Regulatory Affairs*, 24, pp. 1-23. 2007.
DOI: [10.1080/10601330701220520](https://doi.org/10.1080/10601330701220520)
- [20] Guignon, B., Duquenoy, A., Dumoulin, E. D. "Fluid bed encapsulation of particles: principles and practice", *Drying Technol.* 20, pp. 419–447. 2002.
DOI: [10.1081/DRT-120002550](https://doi.org/10.1081/DRT-120002550)
- [21] Cruz, N., Briens, C., Berruti, F. "Supersonic attrition nozzles in gas–solid fluidized beds." *Chemical Engineering and Processing.* 49, pp. 225–234. 2010.
DOI: [10.1016/j.cep.2010.01.010](https://doi.org/10.1016/j.cep.2010.01.010)
- [22] Schaefer, T., Wzrts, O. "pharmaceutical and chemical science." 14, pp. 69-82. 1978.
- [23] Dewettinck, K., Deroo, L., Messens, W., Huyghebaert, A. "Agglomeration Tendency during Top-Spray Fluidized Bed Coating with Gums." *Lebensm.-Wiss. u.-Technol.* 31, pp. 576-584. 1998.
DOI: [10.1006/fstl.1998.0421](https://doi.org/10.1006/fstl.1998.0421)
- [24] Dewettinck, K., Messens, W., Deroo, L., Huyghebaert, A. "Agglomeration Tendency during Top-Spray Fluidized Bed Coating with Gelatin and Starch Hydrolysate." *Lebensm.-Wiss. u.-Technol.* 32, pp. 102-106. 1999.
DOI: [10.1006/fstl.1998.0507](https://doi.org/10.1006/fstl.1998.0507)
- [25] Boerefijn, R., Hounslow, M.J. "Studies of fluid bed granulation in an industrial R&D context." *Chemical Engineering Science.* 60, pp. 3879 – 3890. 2005.
DOI: [10.1016/j.ces.2005.02.021](https://doi.org/10.1016/j.ces.2005.02.021)
- [26] Sau, C., Biswal, K.C. "Computational fluid dynamics and experimental study of the hydrodynamics of a gas–solid tapered fluidized bed." *Applied Mathematical Modelling.* 35, pp. 2265–2278. 2011.
DOI: [10.1016/j.apm.2010.11.037](https://doi.org/10.1016/j.apm.2010.11.037)
- [27] Hede, P., Bach, P., Jensen, A. "Batch top-spray fluid bed coating: Scale-up insight using dynamic heat- and mass-transfer modelling." *Chemical Engineering Science.* 64, pp. 1293 – 1317. 2009.
DOI: [10.1016/j.ces.2008.10.058](https://doi.org/10.1016/j.ces.2008.10.058)

- [28] Rames, C., Zank, J., Martin, M. "Modeling the droplet deposition behavior on a single particle in fluidized bed spray granulation process." Powder Technology. 115. pp. 51-57. 2001.
DOI:[10.1016/S0032-5910\(00\)00279-5](https://doi.org/10.1016/S0032-5910(00)00279-5)
- [29] Heinrich, S., Henneberg, M., Peglow, M., Drechsler, J., Mörl, L. "Fluidized bed spray granulation: analysis of heat and mass transfers and dynamic particle populations". Braz. J. Chem. Eng. 22. No.2. 2005.
DOI: [10.1590/S0104-66322005000200004](https://doi.org/10.1590/S0104-66322005000200004)
- [30] Ratnaparkhi, M., Pandya, V., Chaudhari, S. "Optimization of Various Process Parameters for Formulation of Hypolipidemic Agent by Using Fluid Bed Technology" RJPBCS. 3. No.443. 2012.
- [31] Dybdahl Hede, P., Bach, P., Jensena, A. "Validation of the flux number as scaling parameter for top-spray fluidised bed systems." Chemical Engineering Science. 63. pp. 815 - 828. 2008.
DOI:[10.1016/j.ces.2007.10.017](https://doi.org/10.1016/j.ces.2007.10.017)
- [32] Devi, KDB., Vijayalakshmi, P., Shilpa, V., Prasad T, VSSL., Veerendra Kumar, B., "Response surface methodology for the optimization of kojic acid production by Aspergillus flavus using Palmyra sap as a carbon source." European Journal of Biotechnology and Bioscience. 2 (5). pp. 52-57. 2014.
DOI:[10.1016/j.ejbs.2014.05.019](https://doi.org/10.1016/j.ejbs.2014.05.019)